



An aggregation-induced emissive chromophore as a ratiometric fluorescent sensor for cyanide in aqueous media



Guang-Liang Fu, Cui-Hua Zhao*

School of Chemistry and Chemical Engineering, Shandong University, Jinan 250100, People's Republic of China

ARTICLE INFO

Article history:

Received 27 October 2012

Received in revised form 5 December 2012

Accepted 14 December 2012

Available online 22 December 2012

Keywords:

Intramolecular charge transfer
Aggregation-induced emission
Ratiometric fluorescent sensor
Aqueous media
Cyanide

ABSTRACT

A *para*-terphenyl derivative containing a lateral diphenylamino group and two terminal dicyanovinyl groups has been designed and synthesized. This compound displays aggregation-induced emission characteristics and thus shows intense intramolecular charge transfer fluorescence even in the condensed state, including in the aggregates formed in an aqueous solvent system consisting of greater than 99% water and in the solid state. The addition of cyanide to its aggregates in aqueous media induces a large blue shift in fluorescence, enabling ratiometric fluorescence sensing of cyanide anions. In addition, its prompt fluorescence responses to cyanide anions were also observed even in the solid state.

© 2012 Elsevier Ltd. All rights reserved.

1. Introduction

The sensitive and selective recognition of anions has attracted significant consideration because of their indispensable roles in biological, environmental, and industrial processes.¹ Among various anions, cyanide detection is particularly important due to its extreme toxicity in physiological systems² and the increasing environmental concern caused by its widespread industrial uses in petrochemical, gold mining, photographic, and steel manufacturing.³ To detect cyanide anions, fluorescence sensing is one of the most powerful methods owing to its simplicity and high sensitivity. The conventional fluorescence methodology, which monitors the fluorescence intensity at a single wavelength, is easily interfered by sensor concentration, photobleaching, and illumination intensity. To eliminate these effects, it is desirable to develop a ratiometric fluorescent measurement, which uses the ratio of the fluorescent intensities at two different wavelengths, allowing precise and quantitative analysis and imaging even in complicated systems. Although a variety of fluorescent cyanide sensors have been developed based on reversible binding and reaction-based approaches,^{4,5} the ratiometric fluorescent ones are still quite limited.⁶ Another problem encountered in the fluorescent sensing of cyanide is that most of the fluorescent sensors only function in either pure organic solvents or solutions containing a large amount of organic

solvent, significantly rare in aqueous media.⁷ In this regard, it is still very challenging to obtain ratiometric fluorescent sensor for cyanide, which can be used in aqueous media.

To realize the ratiometric fluorescent sensing of cyanide in aqueous media, one major obstacle is that most organic fluorophores suffer from the aggregation-induced fluorescence quenching phenomenon and are weakly emissive or even non-emissive in water as a result of the aggregates formation. So it is desirable to design the cyanide active fluorophores, which exhibit the aggregation-induced emission characteristics and are highly emissive in aqueous phase despite the formation of aggregates.^{8–10} Herein we designed a new cyanide sensor **1**, a lateral diphenylamino substituted *para*-terphenyl derivative with two dicyanovinyl groups attached at the terminal positions (Fig. 1). In this molecular design, we chose the lateral diphenylamino-substituted *para*-terphenyl system since it has been proved to be an effective strategy to attain intense fluorescence in the condensed state by introduction

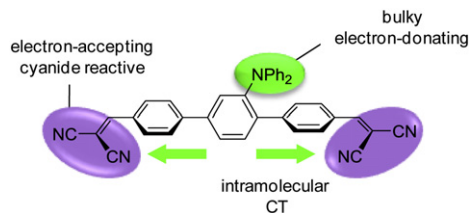


Fig. 1. Molecular design concept of **1**.

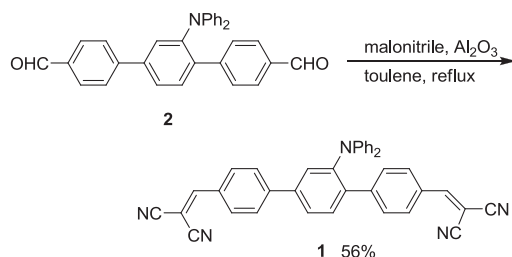
* Corresponding author. Tel.: +86 531 88363756; fax: +86 531 88564464; e-mail address: chzhao@sdu.edu.cn (C.-H. Zhao).

of the bulky electron-donating diphenylamino group at the side position of an electron-accepting *para*-terphenyl framework.¹¹ The dicyanovinyl group was introduced because it can act not only as a strong electron-accepting group to induce an intramolecular charge transfer (ICT) transition but also as a cyanide reactive unit.¹² We envisioned that this molecule would display intense ICT fluorescence even in the aggregates formed in an aqueous media. The nucleophilic attack of cyanide to the α -position of the dicyanovinyl group would disrupt the ICT transition and lead to significant changes in fluorescence, enabling the ratiometric fluorescent sensing of cyanide. We indeed found that compound **1** displays intense fluorescence and prompt ratiometric fluorescent responses to cyanide in an aqueous solvent system consisting of greater than 99% water. Moreover, its intense fluorescence and prompt fluorescence responses to cyanide were also observed even in the solid state.

2. Results and discussion

2.1. Synthesis

Compound **1** was easily synthesized via a one-step reaction as depicted in Scheme 1. In the presence of basic aluminum oxide, the condensation of malonitrile with compound **2**, which was previously prepared through Pd(0)-catalyzed Suzuki–Miyaura coupling of 2,5-dibromo-*N,N*-diphenylaminobenzene with *para*-formylphenylboronic acid,¹¹ provided **1** as yellowish orange solids in 56% yield. Its structure was fully characterized by ¹H NMR, ¹³C NMR spectroscopy, and high-resolution mass spectrometry.



Scheme 1. Synthesis of **1**.

2.2. Photophysical properties

The UV/vis absorption and emission spectra of **1** are shown in Fig. 2 and the related data are summarized in Table 1. In cyclohexane, the absorption of **1** features a much weaker band at the longer wavelength ($\lambda_{\text{abs}}=448$ nm, $\epsilon=2273$ M⁻¹ cm⁻¹) relative to the intense band at 355 nm ($\epsilon=32,350$ M⁻¹ cm⁻¹). In the fluorescence spectra, **1** exhibits an intense emission at 543 nm with a high quantum yield ($\Phi_{\text{F}}=0.56$). It is notable that a large solvatochromism was observed in fluorescence ($\lambda_{\text{em}}=543$ nm in cyclohexane;

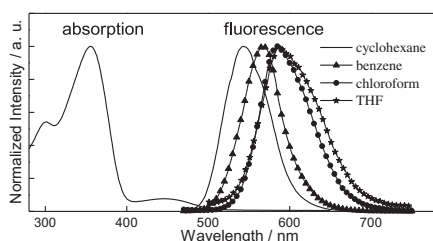


Fig. 2. UV/vis absorption and fluorescence spectra of **1**.

Table 1
UV/vis absorption and fluorescence data of **1** in various solvents

Solvent	λ_{abs} (nm) ^a	ϵ (M ⁻¹ cm ⁻¹)	λ_{em} (nm)	$\Phi_{\text{F}}^{\text{b}}$
Cyclohexane	448	2273	543	0.56
Benzene	446	407	568	0.18
CHCl ₃	458	304	585	0.0047
THF	442	402	589	0.0015
MeCN	442	1462	n.d. ^c	n.d. ^c

^a Only the longest maxima are shown.

^b Calculated using Rhodamine B as standard.

^c Not detected.

568 nm in benzene; 585 nm in CHCl₃; 589 nm in THF) while the absorption spectra display trivial solvent dependence. In addition, the large bathochromism in emission is accompanied by a significant decrease of the fluorescence efficiency with the increasing solvent polarity. And thus the fluorescence in THF ($\Phi_{\text{F}}=0.0015$) is almost invisible to the naked eyes and in MeCN is not detectable even by the spectrometer. These facts clearly suggest a higher polarity in excited state than in the ground state.

To elucidate the influence of the geometric and electronic structure of **1** on photophysical properties, we conducted theoretical calculations. The optimizations of the molecular geometry were carried out using density-functional theory (DFT) at the B3LYP/6-31G(d) level of theory. We also performed time-dependent density-functional theory (TD-DFT) calculations at the B3LYP/6-31G(d) theory. The optimized molecular structure and the pictorial drawing of the molecular orbitals are shown in Fig. 3 and Fig 4, respectively.

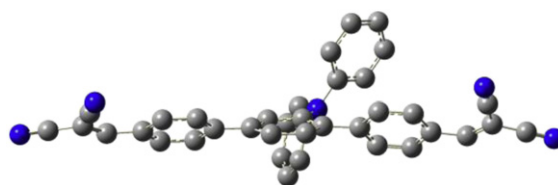


Fig. 3. Optimized structure of **1** calculated at B3LYP(6-31G(d)) theory.

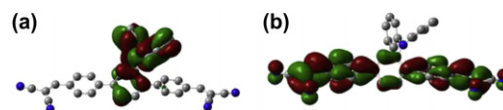


Fig. 4. Pictorial drawings of (a) HOMO and (b) LUMO of **1** calculated at B3LYP/6-31G(d) theory.

As shown in Fig. 3, the terphenylene moiety of **1** shows a non-planar main chain structure, similar to that of the single crystal X-ray structure of other lateral diphenylamino-substituted terphenyl derivatives.¹¹ The dihedral angles between the two terminal benzene rings and the central benzene ring are 34.9° and 47.6°, respectively. Apparently, the difference in the dihedral angles arises from the difference in the steric congestion between the two terminal benzene rings and the central benzene ring. Owing to the twisted main chain structure and the steric hindrance of the lateral diphenylamino group, it is presumed that the molecules of **1** in the condensed state would be far apart from each other, suppressing intermolecular interactions. Another notable feature for the optimized structure of **1** is that the terminal dicyanovinyl groups are almost completely coplanar with the attached benzene rings, suggesting the possible effective conjugation between the

dicyanovinyl groups with the terphenyl main chain framework. As for the electronic structure, compound **1** has a HOMO localized on the central diphenylaminophenylene moiety. It is noteworthy that the LUMO is delocalized over the entire terphenyl framework including the dicyanovinyl unit, indicating the efficient extension of conjugation through the terminal dicyanovinyl groups. The TD-DFT calculations indicate that the weak absorption at the longest wavelength is assignable to an ICT transition from the HOMO to the LUMO. The oscillator strength for the lowest ICT transition is very low ($f=0.0449$), which is consistent with the particularly low intensity of the ICT absorption band. The possible reason is due to the twisted terphenylene framework, which would prevent the occurrence of the ICT transition.

It is intriguing to note that the powder of **1** shows very bright yellowish orange fluorescence despite that it is almost non-emissive in polar solvents (Fig. 5). The quantum yield for the powder of **1** is 0.11, as determined by the calibrated integrating sphere system. The fluorescence efficiency of the powder is almost 100 times higher than that in THF solution, suggesting its high fluorescence efficiency in the condensed state. This observation prompted us to investigate its photophysical properties in aggregates in aqueous media, the intense fluorescence of which would make it possible to realize the ratiometric fluorescence sensing of cyanide in aqueous media. To apply compound **1** efficiently in an aqueous environment, cetyltrimethylammonium bromide (CTAB) was introduced into the aqueous phase due to the insolubility of **1** in water.¹³ The aqueous dispersions were prepared via the rapid injection of a solution of **1** in THF (100 μ L, 4.18 mM) into a micellar aqueous solution of cetyltrimethylammonium bromide (CTAB) (10 mL, 2.0 mM) under vigorous stirring for 30 s. The formation of nanoaggregates was evidenced by the transmission electron microscopy (TEM) images (see Supplementary data), illustrating the morphology of spherical micelles of CTAB, in which compound **1** is presumed to be very concentrated to form aggregates. Notably, the fluorescence intensity increases by more than 10 times once it forms aggregates in CTAB micellar solution relative to that in THF solution, demonstrating the aggregate-induced emission characteristics of **1**. Such fluorescence behavior may be ascribed to the easily exchangeable multiple conformations of the nonplanar structure of the main chain, which facilitate the nonradiative decay of the excited state. In the aggregates, the exchanges between multiple conformations are greatly suppressed due to the spatial congestion of the molecular stacking in the condensed state.^{8–10} The intense emission of **1** in aggregates is also probably ascribed to the efficient ICT transition with large Stokes shift as well as the absence of strong intermolecular interactions, which facilitating the fluorescence quenching in the condensed state.¹¹ In addition, the absence of strong intermolecular interactions was further evidenced by the similarity in the absorption and emission spectra in water compared with those in THF solution.

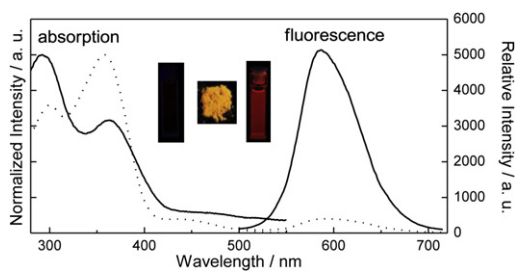


Fig. 5. Absorption and fluorescence spectra of **1** in THF (dotted line), 2 mM CTAB micellar solution (solid line). Inset: photographs of **1** under irradiation of 365 nm, arranged in the following order: in THF, powder and CTAB micellar solution.

2.3. Sensing properties

Considering the intense ICT fluorescence of **1** in aqueous media, we next explored its potential utility as a fluorescent sensor of anions. The fluorescence spectra changes were first examined in the presence of cyanide anions using tetrabutylammonium cyanide (TBACN) as the cyanide source based on the reported fluorescence sensing ability of several dicyanovinyl-containing compounds for cyanide detection.¹² The addition of cyanide to the dispersion of **1** in CTAB micellar solution resulted in a significant blue shift of emission from 590 nm to 450 nm ($\Delta\lambda=140$ nm) immediately. The prompt response of **1** to cyanide in CTAB micelles is possibly ascribed to the electrostatic interactions between anionic cyanide and cationic CTAB, which would attract the cyanide to the micellar surface and thus facilitate the attack of cyanide to **1**.¹³ In addition to the large blue shift, another notable feature in the fluorescence spectral change of **1** in CTAB micellar solution upon addition of cyanide is the significant increase in the fluorescence intensity. The remarkable blue shift and high fluorescence intensity of **1** irrespective of the binding mode suggest its potential ratiometric fluorescence sensing ability for cyanide anions. The titration experiment of **1** with cyanide was carried out and the fluorescence spectral change is shown in Fig. 6. As the concentration of cyanide increased, the emission band at 590 nm decreased and the blue-shifted band at 450 nm increased gradually. This change became saturated when the concentration of cyanide amounted to 196 μ M. The presence of a clear isobestic point might suggest that only one new species was formed during the titration process. Fig. 7 shows a correlation between intensity ratios of fluorescence intensity at 450 nm with those at 590 nm versus cyanide concentration. It is noteworthy that the ratios of emission intensities at 450 and 590 nm (I_{450}/I_{590}) exhibit a dramatic change from 0.19:1 to 23.8:1, demonstrating the ratiometric fluorescent sensing ability of **1** for cyanide detection in CTAB micellar solution, a solvent system consisting of greater than 99% water. Moreover, a dramatic color change of emission was observed from orangish red to blue, thus enabling colorimetric cyanide ion sensing by the naked eyes. Despite the utilization of several dicyanovinyl-based fluorescent

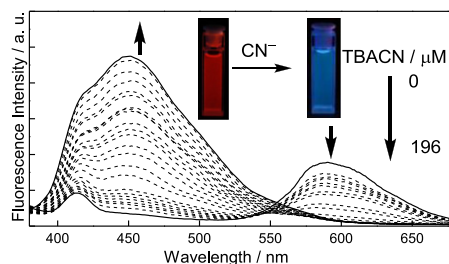


Fig. 6. Fluorescence spectra change of **1** (2.80 μ M) in 2 mM CTAB micellar solution upon addition of TBACN ($\lambda_{\text{ex}}=370$ nm). Inset: emission color change upon addition of TBACN.

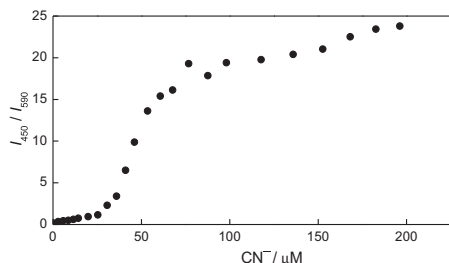


Fig. 7. Plot of fluorescence intensity ratios between 450 and 590 (I_{450}/I_{590}) versus concentration of CN^- in 2 mM CTAB micelles.

sensors for cyanide detection,¹² their ratiometric fluorescent sensing of cyanide in an aqueous media consisting of greater than 99% water has been unprecedented so far.

In the design of cyanide sensor, the interference by other anions, such as fluoride and acetate is a serious challenge. To evaluate the sensing selectivity of **1**, fluorescence changes upon addition of various anions including fluoride (F^-), chloride (Cl^-), bromide (Br^-), iodide (I^-), dihydrogenphosphate ($H_2PO_4^-$), nitrite (NO_2^-), nitrate (NO_3^-), hydrocarbonate (HCO_3^-), bisulfate (HSO_4^-), perchlorate (ClO_4^-), acetate (AcO^-) were evaluated. In contrast to the remarkable fluorescence change with the reaction of **1** with cyanide anion, no obvious fluorescence changes were observed for these anions. In addition, the fluorescence ratio data (I_{450}/I_{590}) is in good consistence with results of the emission spectra (Fig. 8), indicating the high sensing selectivity of **1** toward cyanide over other anions. This is reasonable considering the stronger nucleophilicity of cyanide compared with other anions.

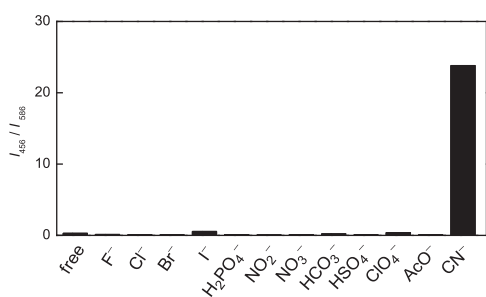


Fig. 8. The fluorescence intensity ratio (I_{450}/I_{590}) response profiles of **1** ($2.80 \mu M$) upon addition of various anions (0.30 mM) in 2 mM CTAB micellar solution ($\lambda_{ex}=370 \text{ nm}$).

The realization of solid state detection is quite meaningful for the sensor in its practical application in portable sensing devices. To facilitate the use of **1** for the detection of cyanide, we prepared test papers of **1** by dipping a filter paper into the solution of **1** in THF ($2.8 \mu M$) following by exposing it to air to dry it.^{13a,14} The fluorescence color didn't show any change if the test paper was immersed in an aqueous solution of cyanide (0.3 mM) in water. Intriguingly, the emission color changed immediately from red to blue once the test paper was immersed into an aqueous solution (0.3 mM) of cyanide in CTAB micelles (Fig. 9), suggesting important role of CTAB to promote the interactions between the cyanide and compound **1**. Thereby compound **1** exhibits excellent fluorescence sensing performance even in the solid state, which will be very useful for the fabrication of sensing devices with fast and convenient detection for cyanide and ions.

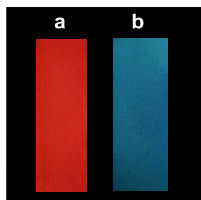


Fig. 9. Photographs of **1** on test papers (a) before and after (b) immersion into aqueous solutions with CN^- (0.3 mM) under irradiation at 365 nm .

To investigate the mechanism of **1** in sensing of cyanide, its 1H NMR spectral changes induced by the addition of cyanide anions were measured in $CDCl_3$ at room temperature. As shown in Fig 10, all of the aromatic proton signals assigned to the terminal phenyl rings are up-field shifted after addition of cyanide. In addition, the olefinic protons at 7.96 and 7.99 ppm are weakened simultaneously

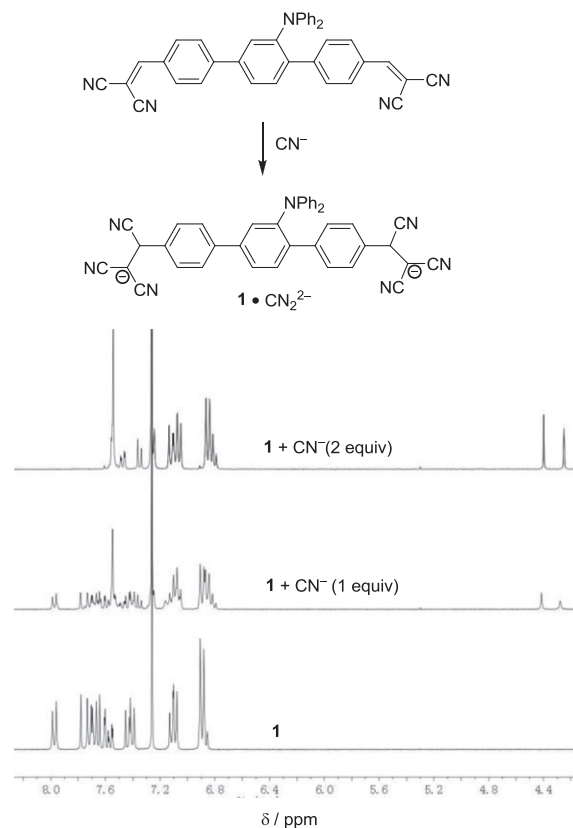


Fig. 10. Partial 1H NMR spectra (300 MHz , $CDCl_3$) of **1** (4.54 mM) with CN^- (as TBA salt).

upon addition of 1 equiv cyanide and disappeared completely when 2 equiv cyanide anions were added while two new signals at 4.28 and 4.21 ppm arose at the same time. Interestingly, no signals assignable to the β -protons of the malonitrile groups developed. These observations clearly suggest that two cyanide anions are added simultaneously to the α -position of the dicyanovinyl groups via a nucleophilic conjugate addition and that only one stable anionic species $1 \bullet CN_2^{2-}$ was formed during the titration. The formation of the sole species $1 \bullet CN_2^{2-}$ and the absence of $1 \bullet CN^-$ are consistent with the presence of only one clear isobestic point in the fluorescence spectra titration. Due to the conjugate nucleophilic addition of cyanide to the terminal dicyanovinyl groups, the conjugation between the dicyanovinyl groups and terphenyl framework is interrupted, which would disrupt the ICT transition and thus induce significant hypsochromic shift in fluorescence.

3. Conclusion

In summary, we have disclosed a novel lateral diphenylamino group substituted *para*-terphenyl **1** containing anion-reactive dicyanovinyl groups at terminal positions. This compound displayed intense ICT fluorescence in the condensed state, including in the aggregates formed in aqueous CTAB micelles and in the solid state. The nucleophilic attack of cyanide to the dicyanovinyl group induces the remarkable fluorescence spectra and color changes, enabling ratiometric and colorimetric fluorescent sensing of cyanide anions in an aqueous solvent system consisting of greater than 99% water. Moreover, this compound also shows prompt fluorescence responses to cyanide anions even in the solid state, allowing the uses of the easy-to-prepare test paper for the convenient detection of cyanide anions in daily applications. Our results have not only provided a successful example of the ratiometric fluorescent sensor for

cyanide in aqueous media, but also demonstrated a successful example for the application of our π -conjugated molecules, which exhibit intense fluorescence even in the condensed state by introduction of bulky electron-donating groups at the side positions of electron-accepting framework. Further design of functional emissive materials utilizing this molecular design concept to explore their potential applications in other fields is underway in our group.

4. Experimental section

4.1. General

^1H and ^{13}C NMR spectra were recorded with a Bruker 300 spectrometer. The ESI mass spectra were measured on an Agilent Q-TOF6510 spectrometer. Melting points (mp) were measured on a TECH XT-4 instrument. UV–vis absorption spectra and fluorescence spectra measurement were performed with a Hitachi UV-4100 spectrophotometer and a Perkin Elmer LS-55 Luminescence spectrometer, respectively. The TEM measurement was carried out using a JEM-1400 transmission electron microscope at 120 kV. The reaction for the preparation of **1** was carried out under nitrogen atmosphere. Compound **2** was synthesized according to the literature.¹¹

4.2. Computational methods

All calculations were conducted by using Gaussian 09 program.¹⁵

4.3. Synthesis of compound 1

To a mixture of **2** (140 mg, 0.31 mmol), malonitrile (122 mg, 1.86 mmol), and basic aluminum oxide (316 mg, 3.1 mmol) was added dehydrated toluene 15 mL. The resulting mixture was refluxed under N_2 overnight. After filtration to remove basic aluminum oxide, the mixture was concentrated under reduced pressure. The resulting crude product was subjected to a silica gel column chromatography (1/2 petroleum ether/ CH_2Cl_2), ($R_f=0.31$) to afford 96 mg (0.41 mmol) of **1** in 56% yield as orange solids: mp 304–307 °C; ^1H NMR (CDCl_3 , 300 MHz): δ 6.84–6.90 (m, 6H), 7.07–7.12 (m, 4H), 7.38–7.44 (m, 3H), 7.54–7.77 (m, 8H), 7.95 (d, $J=8.4$ Hz, 2H); ^{13}C NMR (CDCl_3 , 400 MHz): δ 82.2, 82.6, 112.61, 112.63, 113.6, 113.7, 122.3, 122.4, 124.2, 127.8, 127.9, 129.0, 129.5, 129.6, 130.2, 130.4, 131.3, 132.3, 138.1, 140.7, 145.6, 145.8, 146.2, 147.0, 158.8, 159.1; HRMS (EI): 550.2032 ($[\text{M}+\text{H}]^+$); calcd for $\text{C}_{38}\text{H}_{24}\text{N}_5$: 550.2059.

Acknowledgements

We are grateful for the financial support from the National Natural Science Foundation of China (grant nos. 21072117, 21272141) and 973 program (grant no. 2010CB933504).

Supplementary data

Supplementary data associated with this article can be found in the online version, at <http://dx.doi.org/10.1016/j.tet.2012.12.034>. These data include MOL files and InChIKeys of the most important compounds described in this article.

References and notes

- (a) Beer, P. D.; Gale, P. A. *Angew. Chem., Int. Ed.* **2001**, *40*, 486–516; (b) Martínez-Mañez, R.; Sancenón, F. *Chem. Rev.* **2003**, *103*, 4419–4476; (c) Amendola, V.; Esteban-Gómez, D.; Fabbri, L.; Licchelli, M. *Acc. Chem. Res.* **2006**, *39*,

- 343–353; (d) Gale, P. A.; García-Garrido, S. E.; Garric, J. *Chem. Soc. Rev.* **2008**, *37*, 151–190; (e) Gaunlaugsson, T.; Glynn, M.; Tocci (née Hussey), G. M.; Kruger, P. E.; Pfeffer, F. M. *Coord. Chem. Rev.* **2006**, *250*, 3094–3117.
- (a) Kulig, K. W. *Cyanide Toxicity*; U. S. Department of Health and Human Services: Atlanta, GA, 1991; (b) Baskin, S. I.; Brewer, T. G. In *Medical Aspects of Chemical and Biological Warfare*; Sidell, F., Takafuji, E. T., Franz, D. R., Eds.; TMM: Washington, DC, 1997; Chapter 10, pp 271–286.
- (a) Koenig, R. *Science* **2000**, *287*, 1737–1738; (b) Miller, G. C.; Pritsos, C. A. *Cyanide: Soc., Ind. Econ. Aspects, Proc. Symp. Annu. Meet. TMS* **2001**, 73–81; (c) Young, C.; Tidwell, L.; Anderson, C. *Cyanide: Social, Industrial and Economic Aspects*; Mineral, Metals, and Materials Society: Warrendale, 2001.
- (a) Xu, Z.; Chen, X.; Kim, H. N.; Yoon, J. *Chem. Soc. Rev.* **2010**, *39*, 127–137.
- (a) Shiraishi, Y.; Sumiya, S.; Hirai, T. *Chem. Commun.* **2011**, 4953–4955; (b) Ekmekci, Z.; Yilmaz, M. D.; Akkaya, E. U. *Org. Lett.* **2008**, *10*, 461–464; (c) Kim, H. J.; Ko, K. C.; Lee, J. H.; Lee, J. Y.; Kim, J. S. *Chem. Commun.* **2011**, 2886–2888; (d) Park, S.; Kim, H.-J. *Sens. Actuators, B* **2012**, *161*, 317–321.
- (a) Saha, S.; Ghosh, A.; Mahato, P.; Mishra, S.; Mishra, S. K.; Suresh, E.; Das, S.; Das, A. *Org. Lett.* **2010**, *12*, 3406–3409; (b) Yuan, L.; Lin, W.; Yang, Y.; Song, J.; Wang, J. *Org. Lett.* **2011**, *13*, 3730–3733; (c) Yu, H.; Zhao, Q.; Jiang, Z.; Qin, J.; Li, Z. *Sens. Actuators, B* **2010**, *148*, 110–116; (d) Chen, C.-L.; Chen, Y.-H.; Chen, C.-Y.; Sun, S.-S. *Org. Lett.* **2006**, *8*, 5053–5056; (e) Divya, K. P.; Sreejith, S.; Balakrishna, B.; Jayamurthy, P.; Anees, P.; Ajayaghosh, A. *Chem. Commun.* **2010**, 6069–6071; (f) Lv, X.; Liu, J.; Liu, Y.; Zhao, Y.; Sun, Y.-Q.; Wang, P.; Guo, W. *Chem. Commun.* **2011**, 12843–12845.
- (a) Kim, Y.; Huh, H.-S.; Lee, M. H.; Lenov, I. L.; Zhao, H.; Gabbai, F. P. *Chem.—Eur. J.* **2011**, *17*, 2057–2062; (b) Jung, H. S.; Han, J. H.; Kim, Z. H.; Kang, C.; Kim, J. S. *Org. Lett.* **2011**, *13*, 5056–5059; (c) Chen, X.; Nam, S.-W.; Kim, G.-H.; Song, N.; Jeong, Y.; Shin, I.; Kim, S. K.; Kim, J.; Park, S.; Joon, J. *Chem. Commun.* **2010**, 8953–8955; (d) Jo, J.; Lee, D. J. *Am. Chem. Soc.* **2009**, *131*, 16283–16291; (e) Lee, K. S.; Kim, H.-J.; Kim, G.-H.; Shin, I.; Hong, J. I. *Org. Lett.* **2008**, *10*, 49–51; (f) Peng, L.; Wang, M.; Zhang, G.; Zhang, D.; Zhu, D. *Org. Lett.* **2009**, *11*, 1943–1946.
- (a) Hong, Y.; Lam, J. W. Y.; Tang, B. Z. *Chem. Soc. Rev.* **2011**, *40*, 5361–5388; (b) Hong, Y.; Lam, J. W. Y.; Tang, B. Z. *Chem. Commun.* **2009**, 4332–4353.
- (a) Chen, J.; Law, C. C. W.; Lam, J. W. Y.; Dong, Y.; Lo, S. M. F.; Williams, I. D.; Zhu, D.; Tang, B. Z. *Chem. Mater.* **2003**, *15*, 1535–1546; (b) Mei, J.; Wang, J.; Sun, J. Z.; Zhao, H.; Yuan, W.; Deng, C.; Chen, S.; Sung, H. H. Y.; Lu, P.; Qin, A.; Kwok, H. S.; Ma, Y.; Williams, I. D.; Tang, B. Z. *Chem. Sci.* **2012**, *3*, 549–558; (c) Liu, Y.; Deng, C.; Tang, L.; Qin, A.; Hu, R.; Sun, J. Z.; Tang, B. Z. *J. Am. Chem. Soc.* **2011**, *133*, 660–663; (d) Yuan, W. Z.; Chen, S.; Lam, J. W. Y.; Deng, C.; Lu, P.; Sung, H. H. Y.; Williams, I. D.; Kwok, H. S.; Zhang, Y.; Tang, B. Z. *Chem. Commun.* **2011**, 11216–11218; (e) Zhao, Z.; Wang, Z.; Lu, P.; Chan, C. Y. K.; Liu, D.; Lam, J. W. Y.; Sung, H. H. Y.; Williams, I. D.; Ma, Y.; Tang, B. Z. *Angew. Chem., Int. Ed.* **2009**, *48*, 7608–7611; (f) Yu, G.; Yin, S.; Liu, Y.; Chen, J.; Xu, X.; Sun, X.; Ma, D.; Zhan, X.; Peng, Q.; Shuai, Z.; Tang, B.; Zhu, D.; Luo, Y. *J. Am. Chem. Soc.* **2005**, *127*, 6335–6346; (g) Luo, J.; Xie, Z.; Lam, J. W. Y.; Cheng, L.; Chen, H.; Qiu, C.; Kwok, H. S.; Zhan, X.; Liu, Y.; Zhu, D.; Tang, B. Z. *Chem. Commun.* **2001**, 1740–1741.
- (a) Zhang, Z.; Xu, B.; Su, J.; Shen, L.; Xie, Y.; Tian, H. *Angew. Chem., Int. Ed.* **2011**, *50*, 11654–11657; (b) Wang, B.; Wang, Y.; Hua, J.; Jiang, Y.; Huang, J.; Qian, S.; Tian, H. *Chem.—Eur. J.* **2011**, *17*, 2647–2655; (c) Kim, S.; Zheng, Q.; He, G. S.; Bharali, D. J.; Pudavar, H. E.; Baev, A.; Prasad, P. N. *Adv. Funct. Mater.* **2006**, *16*, 2317–2323; (d) An, B.-K.; Kwon, S.-K.; Jung, S. D.; Park, S. Y. *J. Am. Chem. Soc.* **2002**, *124*, 14410–14415.
- Zhao, C.-H.; Zhao, Y.-H.; Pan, H.; Fu, G.-L. *Chem. Commun.* **2011**, 5518–5520.
- (a) Lee, C.-H.; Yoon, H.-J.; Shim, J.-S.; Jang, W.-D. *Chem.—Eur. J.* **2012**, *18*, 4513–4516; (b) Liu, Z.; Wang, X.; Yang, Z.; He, W. *J. Org. Chem.* **2011**, *76*, 10286–10290; (c) Cheng, X.; Zhou, Y.; Qin, J.; Li, Z. *ACS Appl. Mater. Interfaces* **2012**, *4*, 2133–2138; (d) Hong, S.-J.; Yoo, J.; Kim, S.-H.; Kim, J. S.; Yoon, J.; Lee, C.-H. *Chem. Commun.* **2009**, 189–191; (e) Lin, Y.-D.; Peng, Y.-S.; Su, W.; Tu, C.-H.; Sun, C.-H.; Chou, T. J. *Tetrahedron* **2012**, *68*, 2523–2526; (f) Cheng, X.; Tang, R.; Jia, H.; Feng, J.; Qin, J.; Li, Z. *ACS Appl. Mater. Interfaces* **2012**, *4*, 4387–4392.
- (a) Hu, R.; Feng, J.; Hu, D.; Wang, S.; Li, S.; Li, Y.; Yang, G. *Angew. Chem., Int. Ed.* **2010**, *49*, 4915–4918; (b) Zhao, Y.; Zhong, Z. *Org. Lett.* **2006**, *8*, 4715–4717; (c) Zhang, X.; Zhang, X.; Wang, S.; Liu, M.; Tao, L.; Wei, Y. *Nanoscale*, <http://dx.doi.org/10.1039/c2nr32698a>.
- (a) Wang, J.; Mei, J.; Yuan, W.; Lu, P.; Qin, A.; Sun, J.; Ma, Y.; Tang, B. Z. *J. Mater. Chem.* **2011**, *21*, 4056–4059; (b) Qin, A.; Lam, J. W. Y.; Tang, L.; Jim, C. K. W.; Zhao, H.; Sun, J.; Tang, B. Z. *Macromolecules* **2009**, *42*, 1421–1424.
- Frisch, M. J.; Trucks, G. W.; Schlegel, H. B.; Scuseria, G. E.; Robb, M. A.; Cheeseman, J. R.; Scalmani, G.; Barone, V.; Mennucci, B.; Petersson, G. A.; Nakatsuji, H.; Caricato, M.; Li, X.; Hratchian, H. P.; Izmaylov, A. F.; Bloino, J.; Zheng, G.; Sonnenberg, J. L.; Hada, M.; Ehara, M.; Toyota, K.; Fukuda, R.; Hasegawa, Y.; Ishida, M.; Nakajima, T.; Honda, Y.; Kitao, O.; Nakai, H.; Vreven, T.; Montgomery, J. A.; Peralta, J. E., Jr.; Ogliaro, F.; Bearpark, M.; Heyd, J. J.; Brothers, E.; Kudin, K. N.; Staroverov, V. N.; Kobayashi, R.; Normand, J.; Raghavachari, K.; Rendell, A.; Burant, J. C.; Iyengar, S. S.; Tomasi, J.; Cossi, M.; Rega, N.; Millam, J. M.; Klene, M.; Knox, J. E.; Cross, J. B.; Bakken, V.; Adamo, C.; Jaramillo, J.; Gomperts, R.; Stratmann, R. E.; Zayzev, O.; Austin, A. J.; Cammi, R.; Pomelli, C.; Ochterski, J. W.; Martin, R. L.; Morokuma, K.; Zakrzewski, V. G.; Voth, G. A.; Salvador, P.; Dannenberg, J. J.; Dapprich, S.; Daniels, A. D.; Farkas, O.; Foresman, J. B.; Ortiz, J. V.; Cioslowski, J.; Fox, D. J. *Gaussian 09, Revision A.02*; Gaussian: Wallingford CT, 2009.